Potential Curves for the Mg^+Rn Complex Including Charge-Transfer States

P. A. Christiansen* and T. M. Moffett

Department of Chemistry, Clarkson University, Potsdam, New York 13699-5810

G. A. DiLabio

Department of Chemistry, Carleton University, 1125 Colonel By Drive, Ottawa, Ontario, Canada K1S 5B6

Received: April 29, 1999; In Final Form: August 2, 1999

The lighter rare gas complexes with Mg^+ are known from both computational and spectroscopic determinations to have weakly bound $^2\Sigma^+$ ground states with much more strongly bound low-lying $^2\Pi_{1/2,3/2}$ excited states. In extensive configuration interaction calculations including large relativistic effects, we show that for Rn the picture is dramatically different with strongly avoided crossings in the $^2\Pi$ curves due to charge-transfer states. The avoided crossings leave the $^2\Pi$ states much more weakly bound. It was found that the lowering of the Rn ionization potential relative to Xe, producing the low-lying states, can be attributed almost entirely to the large spin−orbit splitting of the Rn^+ ^2P states. Variations in crossing interactions are readily explained in terms of two-component spinors.

Introduction

Over the last 5 years, several groups[1−8] have studied the complexes formed by the rare gases, Ar through Xe, with Mg^+, both experimentally and computationally. Duncan and co-workers[1,4,8] used mass-selected photodissociation spectroscopy to determine vibrational constants and dissociation energies for the ground states of the Ne through Xe complexes. They were also able to determine spin−orbit constants for the $^2\Pi$ states and noted that, while the Ne and Ar complex splittings were on the order of magnitude expected from Mg^+, the Kr and Xe splittings were substantially larger. Le Roy[2] has reanalyzed the data from refs 1 and 4, using near-dissociation expansions, to determine spectroscopic constants for both the $^2\Sigma^+$ and $^2\Pi$ states of the Ar through Xe complexes. Nonrelativistic calculations by Bauschlicher and Partridge[3], using core−valence correlation potentials,[9] show very good agreement with the Ar and Kr numbers from Le Roy, adding credibility to that analysis. Breckenridge and co-workers,[5,6] using two-color photoionization, have determined ground state dissociation energies for the Ar through Xe complexes that are consistent with, but presumably more precise than those of Le Roy. In very recent Ar and Xe calculations including relativistic effects, Matsika and Pitzer[7] have shown that the increased splitting seen by Duncan[1,4,8] is due to the admixture (through orthogonalization) of heavy element pπ character to the Mg^+ 3pπ orbitals. For the four complexes studied, the picture that emerges is one of weakly bound $^2\Sigma^+$ ground states with more strongly bound $^2\Pi_{1/2,3/2}$ excited states. These correlate, respectively, to the ^2S and $^2P_{3/2,1/2}$ states of Mg^+. As one proceeds down the series, the bond energy increases are larger for the excited Π states than for the ground states, resulting in smaller Π state T_e values. In addition to the above states, the calculations by Matsika and Pitzer[7] show the expected weakly bound $^2\Sigma^+$ excited states correlating to Mg^+ $^2P_{3/2}$.

To our knowledge, there has been no work, experimental or theoretical, for the corresponding complexes of radon, although within the relativistic effective potential framework used in ref 7, Mg^+Rn is in principle no more computationally difficult than the lighter complexes. It should be noted that relativistic effects in the valence shells, particularly spin−orbit splittings, increase dramatically from Xe to Rn. In addition, an inspection of rare gas ionization potentials (IP) in comparison to Mg reveals that the difference in the Rn and Mg potentials will place the Rn^+ $^2P_{3/2}$ charge-transfer states well below the Mg^+ $^2P_{3/2,1/2}$ asymptotes, making the Mg^+Rn complex an especially intriguing addition to the series.

In the context of relativistic effects, the Ne through Rn IP sequence[10] (shown graphically in Figure 1 along with spin−orbit splittings and pertinent states of Mg^+) deserves some comment. The difference between the Xe and Mg IPs is only 36 165 cm^{-1}, while for Mg^+ the energy difference between the ^2S and $^2P_{1/2}$ states is 35 669 cm^{-1} with the $^2P_{3/2}$ 92 cm^{-1} higher. Consequently, for the Xe complex, the unobserved charge-transfer states sit less than 500 cm^{-1} above the observed $^2\Pi$ asymptotes. In contrast to Mg^+Xe, the Rn−Mg IP difference is 25 023 cm^{-1}, placing the charge-transfer states more than 10 000 cm^{-1} below the $^2\Pi$ asymptotes. In this context, it is interesting to ask how much effect relativity has on the Rn IP. In simple mass−velocity arguments, relativity is assumed to increase binding of s and p subshells, and this is certainly the case for sixth-row $6p_{1/2}$ spinors, but for the filled shell rare gases, the ionization involves the $6p_{3/2}$. Simple numerical SCF[11] calculations for atomic Rn and Rn^+ with the 6p spin−orbit splitting averaged out show a relativistic IP increase of around 800 cm^{-1}. However, with the splitting included, the IP decreases by roughly 10 000 cm^{-1}. The spin−orbit effect is an order of magnitude larger than that of the simple relativistic contraction, and consequently, it is primarily because of the large spin−orbit splitting that the charge-transfer states become important for Mg^+Rn. Note that, while the large spin−orbit splitting places the Rn^+ $^2P_{3/2}$ charge-transfer states well below the Mg^+ ^2P asymptote, it shifts the Rn^+ $^2P_{1/2}$ charge-transfer state up roughly 20 000 cm^{-1} above the Mg^+ ^2P asymptote and at about the same level as the lowest Rn Rydberg states.

* Corresponding author. E-mail: pac@clarkson.edu.

10.1021/jp9914166 CCC: $18.00
Published on Web 10/04/1999

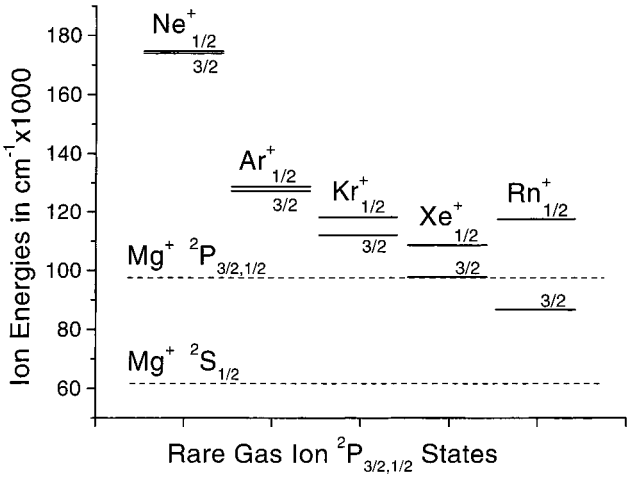

Figure 1. Rare gas $^2P_{3/2}$ and $^2P_{1/2}$ ion energies relative to neutral ground states. The ^2S and ^2P states of Mg^+ have been included for comparison.

TABLE 1: Computed Atomic Excitation Energies in cm^{-1} with Experimental Values for Comparison

state	$R =$ 20.0 bohr	MP, ref 7	Mg^+ ion	expt, ref 10
$^2P_{3/2}$ (Mg^+) + ^1S (Rn)	35 209	35 136	35 806	35 761
$^2P_{1/2}$ (Mg^+) + ^1S (Rn)	35 138	35 052	35 731	35 669
$^2P_{3/2}$ (Rn^+) + ^1S (Mg)	25 298			25 023
$^2S_{1/2}$ (Mg^+) + ^1S (Rn)	0	0	0	0

In the following sections, we present the results of multireference configuration interaction (CI) calculations, including relativistic effects, for the six lowest states of the Mg^+Rn complex.

Calculations and Results

Relativistic effective potentials for Mg and Rn were taken from Christiansen and co-workers.[12,13] For Mg, all but the 1s shell were included in the valence space, while for Rn the 5d, 6s, and 6p were treated in the valence space. The primitive (6s 4p) Mg basis set from ref 12 was augmented with two additional p functions (0.18 and 0.06) to more accurately describe the 3p orbitals and a single d function (3.5297) and was then contracted to (4s 4p 1d). For Rn, the primitive (5s 5p 5d) basis from ref 13 was augmented by a single f function (1.8) and contracted to (3s 4p 4d 1f). Orbitals used in the configuration interaction calculations were taken from ground-state SCF calculations followed by an IVO optimization[14] as in Matsika et al. Double group CI calculations were carried out using the unitary group code recently developed by Yabushita et al.[15] The CI employed seven references representing the four Mg^+ asymptotes and the three Rn^+ charge-transfer asymptotes corresponding to the elimination of an electron from each of the three Rn 6p spinors. Single and double promotions from all orbitals except the filled d shell on Rn were allowed, resulting in more than 2 million double group configurations.

To get a rough gauge of the adequacy of our basis sets and correlation treatment, we computed atomic excitation energies at an internuclear separation of 20.0 bohr (10.58 Å). These are shown in Table 1, along with experimental values as well as values from ref 7. The agreement with values from ref 7 is very good, suggesting a nearly equivalent treatment at the separated atom limit. The agreement with experiment is not nearly so good but is probably adequate for our purposes, with errors in the neighborhood of 600 cm^{-1} or smaller. In particular, there appears to be a reasonable balance of treatments between the Mg and Rn. As can be seen from the table, an additional calculation for Mg^+ alone using the same basis set and excitation level as in the complex, but with only the four Mg^+ references, gives errors about an order of magnitude less, suggesting that the majority of the error in the complex is due to neglect of higher excitations in the molecular CI.

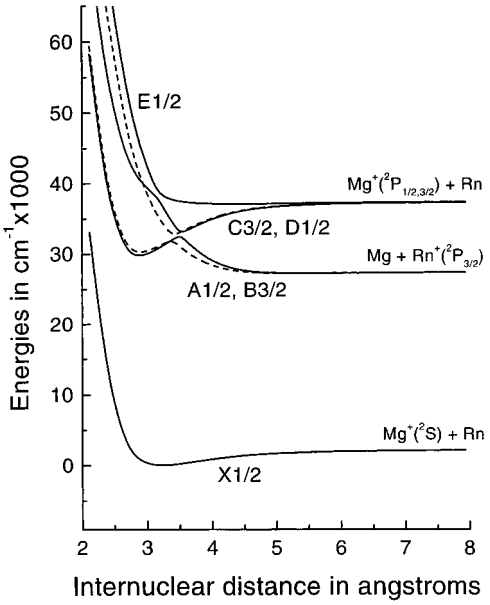

Figure 2. Potential energy curves for the Mg^+Rn complex. The solid lines are for $\Omega = 1/2$ states, while the dashed lines are for $\Omega = 3/2$ states.

TABLE 2: Properties for the Six Lowest Lying States of Mg^+Rn

state	R_e (Å)	D_e (cm^{-1})	ω_e (cm^{-1})	T_e (cm^{-1})
E 1/2	4.41	283	22	36 988
D 1/2	3.56	4221	349	33 046
C 3/2	3.42	4565	362	32 772
B 3/2	2.90	−2829[a] (7080)[b]	222	30 257
	5.44	219	24	27 208
A 1/2	2.88	−2353[a] (7488)[b]	231	29 778
	5.54	257	29	27 169
X 1/2 ($^2\Sigma^+_{1/2}$)	3.24	2129	114	0

[a] Relative to the Rn^+ $^2P_{3/2}$ asymptote. [b] Relative to the Mg^+ $^2P_{3/2,1/2}$ asymptotes, for comparison with the lighter rare gas complexes.

Computed energy curves for the Mg^+Rn complex are shown in Figure 2. The big difference between radon and the lighter rare gases, the presence of low-lying charge-transfer states, is clearly visible in the plot. As can be seen, the resulting avoided crossings give rise to double minima in what would normally be the $^2\Pi$ curves and two sharp minima in the separated upper $^2\Pi$ curves. Properties are shown in Table 2.

Discussion

While the charge-transfer states and their associated avoided crossing significantly disrupt the overall picture relative to the lighter rare gas complexes, the crossings occur some distance from the minima, and so it is reasonable to compare some Mg^+-Rn properties with those of the lighter complexes. However in making such comparisons, especially with experimental values, one must keep in mind the incompleteness of the present correlation treatments and the effects that will have on properties. The correlation treatment used in the present work is on about the same level as that of ref 7, except for the inclusion of d functions on Mg and double promotions from the Mg 2s and 2p subshells, as opposed to singles in ref 7, so a brief look at their results is in order.

TABLE 3: Comparison of the Available Computed and Experimentally Determined Properties for the $^2\Pi_{1/2}$ States of the Mg^+RG Complexes (Energies in cm^{-1}, Bond Lengths in Å)

	T_e or (υ_{00})	R_e or (R_0)	D_e or (D_0)	$^2\Pi$ splitting	ref
Ne	(34 086)	2.59[a]	1804	63	8 (expt)
Ar	32 215	2.54	3363	68	7
	(31 585)	(2.406)	(5097)		3
	(31 396)		(5554)	76	1 (expt)
			(5445)		2 (expt)
Kr	(30 494)	(2.527)	(7020)		3
	(30 464)		(7128)	144	1 (expt)
			(6948)		2 (expt)
Xe	30 051	2.79	6479	288	7
	(28 825)		(11026)	268	1 (expt)
			(10019)		2 (expt)
Rn (A 1/2)	29 778	2.88	7488[b]	408	present

[a] Bond length is R_9. [b] Relative to the Mg^+ $^3P_{1/2}$ asymptote. See Table 2 and Figure 2.

Matsika and Pitzer found the bonding in Mg^+Kr and Mg^+-Xe to be primarily inductive, but with substantial dispersion interactions, particularly apparent in the Σ states. Their analysis seems consistent with the present Mg^+Rn results. Their correlation treatments gave bond lengths too long for the Σ states relative to the available experimental result but were much more reasonable for the Π states (they were concerned primarily with the $^2\Pi$ spin−orbit splittings) with errors in the neighborhood of +0.1 Å or so. In terms of bond energies, they were able to recover over 40% of the experimental values for the Σ states and more than 60% for the Π states. Because of the slightly better treatment of the $n = 2$ shell on Mg, we would expect errors in the present Mg^+Rn bond lengths to be in the neighborhood of 0.1 to 0.2 for the Σ states and perhaps half that magnitude for the Π states, and our corresponding bond energies are expected to be between about 50% and 70% of experiment.

The difference in correlation treatments noted in the previous paragraph almost certainly accounts for the fact that our Σ state bond lengths for Mg^+Rn are actually shorter than the corresponding Mg^+Xe bonds in ref 7. On the basis of the above discussion, we would expect an Mg^+Rn ground-state bond length between 3.1 and 3.2 Å and a bond energy from 3000 to 4000 cm^{-1}. We would expect these correlation differences to have much smaller effects on the Π states so a more direct comparison is reasonable. In Table 3, we list available $^2\Pi_{1/2}$ properties for the Mg^+RG sequence from Ne through Rn. For Rn, we have used the inner minimum from the A 1/2 curve, and for purposes of comparison, report the dissociation energy as it would be in the absence of the charge-transfer states. The table shows clearly the steady rise in spin−orbit splittings, as expected from ref 7, as well as the trend toward increasing bond lengths. On the other hand, our bond strength is not much larger than that from ref 7, despite the slightly improved correlation treatment, and our computed T_e differs inconsequentially from that of ref 7. On the basis of the earlier correlation discussion, we would expect the actual "dissociation" energy to be between 10 000 and 11 000 cm^{-1}. Using our earlier estimate for the ground-state bond, we would expect the "real" T_e value to be near 28 500 cm^{-1}. Neither of these two, T_e or D_e, differs significantly from those of the xenon complex. We would expect the bond length for the A 1/2 state (and B 3/2 as well) to be between 2.8 and 2.9 Å.

Note that in Table 2 the inner wells of the A 1/2 and B 3/2 states are unbound by 2353 and 2829 cm^{-1}, respectively. If our errors due to incomplete correlation are as large as 3000 cm^{-1}, as we expect they are, then both states will be bound with respect to the charge-transfer asymptote, but only barely.

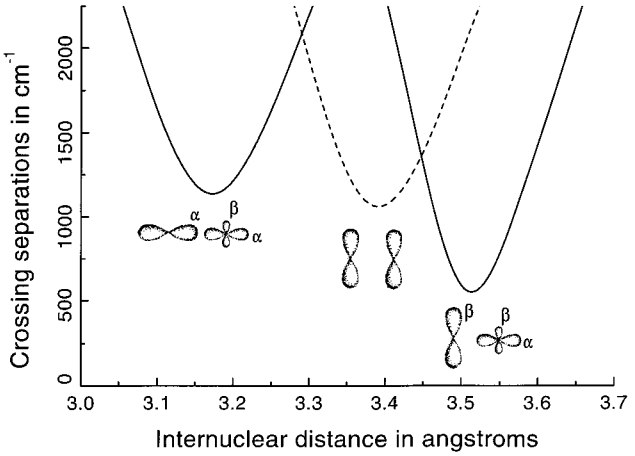

Figure 3. Avoided crossing separations along with corresponding coupling cartoons. The solid lines indicate $\Omega = 1/2$ states, while the dashed line indicates $\Omega = 3/2$. The cartoons below the minima illustrate the dominant spin−orbital/spinor interaction for each avoided crossing. The α and β indicate spin for the $\Omega = 1/2$ curves.

In very recent work on the Mg^+Ne complex using photodissociation spectroscopy, Duncan and co-workers[8] have commented on the persistence of Λ−S (Hund's case *a*) coupling in the observed vibrational levels for the $^2\Pi$ states. They saw nearly constant spin−orbit splittings (63.4 to 62.5 cm^{-1}) even for levels within approximately 100 cm^{-1} of dissociation. In the present Mg^+Rn work, we note that the transition between Λ−S and ω−ω (Hund's case *c*) coupling in the $^2\Pi$ states (C 3/2 and D 1/2) occurs around 6.0 Å, only 120 cm^{-1} or so below the dissociation limit. Furthermore, one can see the beginning of the transition even at 8.0 Å.

An interesting feature of Figure 2 is the large difference in magnitude of the separations in the $\Omega = 3/2$ and $\Omega = 1/2$ avoided crossings arising from the interaction between what would normally be the $^2\Pi$ states and the charge-transfer states. The energy separation for the $\Omega = 3/2$ states is roughly twice that of the $\Omega = 1/2$ states. The $^2\Pi$ states arise from open shells on Mg and are very nearly Λ−S coupling in nature, while the charge-transfer states are due to open shells on the heavy atom. The coupling arises primarily from the interaction between a single spin−orbital in the $^2\Pi$ states and a single spinor for the charge-transfer states. While the $\Omega = 3/2$ spinor is dominated by π character, the $\Omega = 1/2$ spinor is a mixture of σ and π character in a ratio of roughly $2^{1/2}$. In Figure 3, we have plotted the avoided crossing separations and have included "cartoons" of the spinor/spin−orbital configurations in each case. For the $\Omega = 3/2$ states, the interaction is between regular π functions on both centers, while for $\Omega = 1/2$, it involves a π function on Mg and a mostly σ function on the Rn. As a consequence, the $\Omega = 3/2$ separation is roughly twice that of the $\Omega = 1/2$ separation. On the other hand, the innermost $\Omega = 1/2$ avoided crossing involves a σ spin−orbital on Mg and the predominantly σ spinor on Rn, hence the larger magnitude.

Summary

CI calculations for the Mg^+Rn complex, including spin−orbit coupling, show a very different picture from that of the lighter rare gas complexes of Mg^+. Charge-transfer states resulting from the promotion of a Rn $6p_{3/2}$ electron to the Mg 3s subshell introduce avoided crossings in the $^2\Pi$ states (A 1/2 and B 3/2 in our designation) that arise from the Mg^+ $^2P_{1/2,3/2}$ ion states.

As a consequence, the $^2\Pi$ states are essentially unbound in the radon complex. Our calculations suggest that the trend of rapidly increasing bond strengths in both the ground $^2\Sigma^+$ states and the excited $^2\Pi$ states, as seen in the Ar through Xe series of complexes, does not continue for radon. To within the accuracy of our calculations, the ground-state dissociation energy and T_e values for the $^2\Pi$ states do not differ significantly from those of the xenon complex. On the other hand, the increasing splitting of the $^2\Pi$ states does continue, with the Mg^+Rn value being roughly 50% larger than that of Mg^+Xe.

Acknowledgment. This work was completed while one of the authors (P.A.C.) was on sabbatical leave. We greatly appreciate generosity shown by Clarkson University Chemistry Chairman S. E. Friberg, Dean of Science J. H. Thorp, and Academic Vice President A.G. Collins in awarding the sabbatical. We also thank the Department of Chemistry at The Ohio State University, and in particular Prof. R. M. Pitzer, for their generous hospitality throughout the sabbatical stay. We are especially indebted to Prof. Pitzer as well as S. Matsika and S. Brozell for their many useful comments on this work and for allowing the use of their already taxed computational resources. Finally, we acknowledge the use of computational facilities at the Ohio Supercomputer Center.

References and Notes

(1) Pilgrim, J. S.; Yeh, C. S.; Berry, K. R.; Duncan, M. A. *J. Chem. Phys.* **1994**, *100*, 7945.
(2) Le Roy, R. J. *J. Chem. Phys.* **1994**, *101*, 10217.
(3) Bauschlicher, C. W., Jr.; Partridge, H. *Chem. Phys. Lett.* **1995**, *239*, 241.
(4) Scurlock, C. T.; Pilgrim, J. S.; Duncan, M. A. *J. Chem. Phys.* **1995**, *103*, 3293.
(5) Massick, S.; Breckenridge, W. H. *Chem. Phys. Lett.* **1996**, *257*, 465.
(6) Kaup, J. G.; Breckenridge, W. H. *J. Chem. Phys.* **1997**, *107*, 2180.
(7) Matsika, S.; Pitzer, R. M. *J. Phys. Chem.* **1998**, *A102*, 1652.
(8) Reddec, J. E.; Duncan, M. A. *J. Chem. Phys*. **1999**, *110*, 9948.
(9) Muller, W.; Flesch, J.; Meyer, W. *J. Chem. Phys.* **1984**, *80*, 3297.
(10) Moore, C. E. *Atomic Energy Levels*; National Bureau of Standards Circular 467; Volume I, 1949; Volume II, 1952; Volume III, 1958.
(11) Desclaux, J. P. *Comput. Phys. Commun.* **1975**, *9*, 31.
(12) Pacios, L. F.; Christiansen, P. A. *J. Chem. Phys.* **1985**, *82*, 2664.
(13) Wildman, S. A.; DiLabio, G. A.; Christiansen, P. A. *J. Chem. Phys.* **1997**, *107*, 9975.
(14) Hunt, W. J.; Goddard, W. A., III. *Chem. Phys. Lett.* **1969**, *3*, 414.
(15) Yabushita, S.; Zhang, Z.; Pitzer, R. M. *J. Phys. Chem A* **1999**, *103*, 5791.